Thermochimica Acta 480 (2008) 10–14

Contents lists available at ScienceDirect

Thermochimica Acta

journal homepage: www.elsevier.com/locate/tca

Thermal reactions of lithiated graphite anode in $LiPF_6$-based electrolyte

Nam-Soon Choi*, Irina A. Profatilova, Sung-Soo Kim, Eui-Hwan Song

Energy Laboratory, Corporate R&D Center, Samsung SDI Co. Ltd., 575 Shin-dong, Yeongtong-gu, Suwon-si, Gyeonggi-do 443-731, Republic of Korea

ARTICLE INFO

Article history:
Received 30 June 2008
Received in revised form
22 September 2008
Accepted 23 September 2008
Available online 30 September 2008

Keywords:
Thermal decomposition
Lithiated graphite anode
$LiPF_6$
FT-IR
DSC

ABSTRACT

The thermal reactions of a lithiated graphite anode with and without 1.3 M lithium hexafluorophosphate ($LiPF_6$) in a solvent mixture of ethylene carbonate (EC) and ethylmethyl carbonate (EMC) were investigated by means of differential scanning calorimetry (DSC). The products of the thermal decomposition occurring on the lithiated graphite anode were characterized by Fourier transform infrared (FT-IR) analysis. The lithiated graphite anode showed two broad exothermic peaks at 270 and 325 °C, respectively, in the absence of electrolyte. It was demonstrated that the first peak could be assigned to the thermal reactions of PF_5 with various linear alkyl carbonates in the solid electrolyte interphase (SEI) and that the second peak was closely related to the thermal decomposition of the polyvinylidene fluoride (PVdF) binder. In the presence of electrolyte, the lithiated graphite anode showed the onset of an additional exothermic peak at 90 °C associated with the thermal decomposition reactions of the SEI layer with the organic solvents.

1. Introduction

The safety of Li-ion cells is mainly governed by the thermal reactivity of the battery components [1]. Understanding the thermal decomposition reactions of electrolytes, anodes, and cathodes at high temperatures is essential for the design of safe and high performance Li-ion batteries. It is well known that the thermally unstable lithiated graphite anodes and $LiPF_6$-based electrolytes can lead to Li-ion cell safety issues [2–4]. The decomposition of the solid electrolyte interphase (SEI) layer that results from the electrochemically reductive decompositions of the electrolyte on the graphite anode can initialize some exothermic reactions between the lithiated graphite anode and the electrolyte [5]. When a cell is heated above a certain temperature, exothermic chemical reactions between the electrodes and the electrolyte can take place and lead to an increase of the cell internal temperature. If the generated heat is greater than the energy that can be dissipated, exothermic processes will occur and the cell temperature will increase rapidly. This temperature growth will accelerate chemical reactions and lead to the production of even more heat, eventually resulting in the thermal runaway of batteries. Most studies have, so far, focused on the thermal behavior (temperature onset, temperature peak, heat evolution) of various electrolytes [6], lithiated anodes [7–9], and delithiated cathodes [10]. In order to investigate the exothermic peaks observed in thermogravimetry (TG) and derivative thermal analysis (DTA) profiles, Yang et al. monitored the evolution of the gas products as a function of the temperature and weight variation and they proposed different possible reaction pathways [11]. Howard et al. investigated thermal reactions of lithiated graphite anode and delithiated cathode with and without an electrolyte using ARC and DSC-TG. Their results are very informative to understand thermal behaviors of cell components (anode, cathode, and electrolyte). However, the characterization for decomposition products at elevated temperatures was not carried out to explain the mechanism of battery thermal runaway in detail [12] There is no rigorous Fourier transform infrared (FT-IR) analysis available to characterize each exothermic peak on the differential scanning calorimetry (DSC) thermograms. There are some possible exothermic reactions that trigger thermal runaway, including the thermal decompositions of the electrolyte, the reductions of the electrolyte by the anode, the oxidations of the electrolyte by the cathode, the thermal decompositions of the anode and cathode, the melting of the polyolefin separator, and the consequent internal short.

The present work aims to understand the thermal decomposition reactions of lithiated graphite anode with and without an electrolyte solution. We have conducted a detailed investigation of the thermal decomposition products by means of vibrational spec-

* Corresponding author. Tel.: +82 31 210 7575; fax: +82 31 210 7555.
E-mail address: ns75.choi@samsung.com (N.-S. Choi).

0040-6031/$ – see front matter © 2008 Elsevier B.V. All rights reserved.
doi:10.1016/j.tca.2008.09.017

troscopy because of the amount of structural information that can be readily obtained using this technique.

2. Experimental

The electrolyte solution is composed of a commercially available 1.3 M lithium hexafluoro phosphate ($LiPF_6$) dissolved in a solvent mixture of ethylene carbonate (EC) and ethylmethyl carbonate (EMC) with a 3:7 volume ratio. To evaluate the thermal properties of the lithiated graphite anodes, a slurry was prepared by mixing 97 wt.% of graphite particles constituting the active material and 3 wt.% of a polyvinylidene fluoride (PVdF) binder dissolved in anhydrous *N*-methyl-2-pyrrolidinone (NMP). The resulting slurry was cast on a copper foil. The composite electrode was then dried in a convection oven at 110 °C for 2 h. The electrode was next pressed and its thickness was around 40 μm.

Thermal analyses of lithiated graphite anodes and electrolytes were conducted by using a differential scanning calorimetry technique (DuPont TA 2000 DSC). Each sample was sealed in a hermetic stainless steel pan and scanned at a heating rate of 10 °C min^{-1} within an appropriate temperature range under a nitrogen atmosphere.

FT-IR spectra of samples obtained from lithiated graphite anodes heated to various temperatures, electrolytes, organic solvents, and $LiPF_6$ salt were recorded from transmission measurements in a Nicolet NEXUX 870 spectrometer with a spectral resolution of 4 cm^{-1} under a nitrogen atmosphere. After the cells were charged to 0.01 V vs. Li/Li^+, they were carefully opened in a dry room and the electrodes were subsequently rinsed in a dimethyl carbonate (DMC) solvent in order to remove the residual electrolyte. They were then dried under vacuum.

A coin-type half cell with a graphite anode and a Li counter electrode was used in all experiments and assembled in an Ar-filled glove box with less than 1 ppm of both oxygen and moisture. Charge experiments were galvanostatically performed at a rate of 0.1 °C using a computer-controlled battery measurement system (TOSCAT 3000 U).

3. Results and discussion

Fig. 1 presents the DSC heating curves for a $LiPF_6$ salt, a lithiated graphite anode powder, and a lithiated graphite anode with $LiPF_6$. After the cells were charged in EC/EMC (3/7) with 1.3 M $LiPF_6$, they were carefully opened in a dry room. The lithiated graphite anodes were subsequently rinsed in a dimethyl carbonate (DMC) solvent to remove the residual electrolyte and they were finally dried. The thermal properties of the resulting anodes were measured. The specific charge capacity of the graphite anode was approximately of 370 mAh g^{-1} at a charge cut-off potential of 0.01 V vs. Li/Li^+. $LiPF_6$ enclosed in a sealed stainless steel pan shows a sharp endothermic peak at around 197 °C and a broad endothermic peak with a peak temperature of 290 °C, as shown in Fig. 1(a). It is clear that the first peak and the second endothermic peak are attributed to the melting and the thermal decomposition of $LiPF_6$ ($LiPF_6$ (s) ↔ LiF (s) + PF_5 (g)), respectively [13]. An additional small endothermic peak related to the hydrogen fluoride (HF) removal from $LiPF_6$ appears at about 64 °C in Fig. 1(e). Yang et al. reported that the HF free acid is inevitably left over during the salt production and the amount of acid depends on the production technology [14]. The DSC curve (b) for a lithiated graphite anode without electrolyte shows two broad exothermic peaks at 270 and 325 °C. In an attempt to characterize these two exothermic peaks, FT-IR analyses were performed at various temperatures (before heating, 200, 275 and 400 °C). The ex situ FT-IR spectra of the lithiated graphite anode

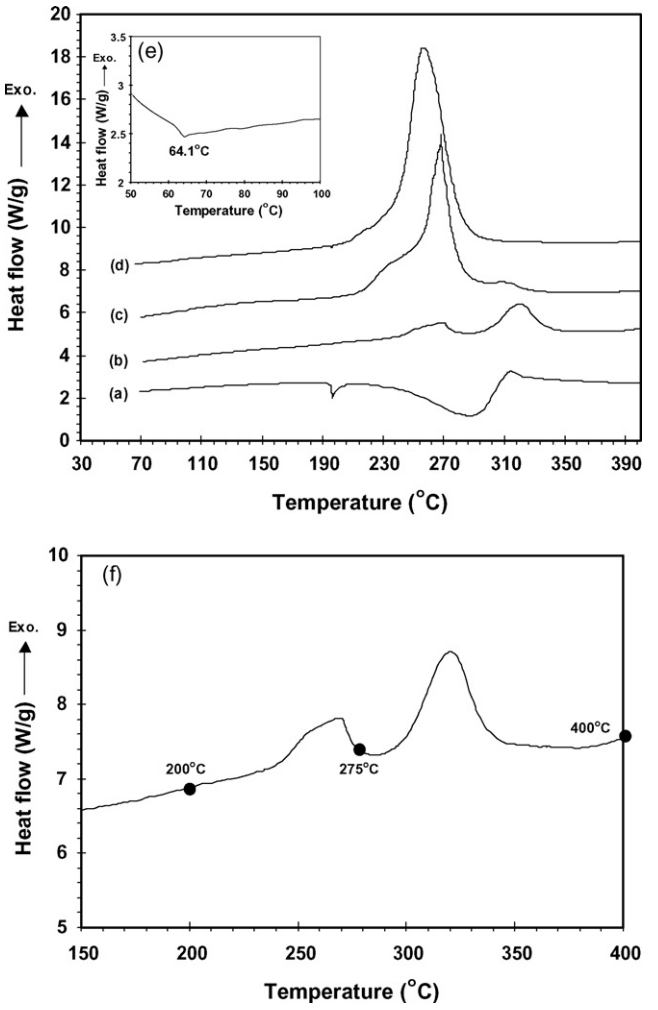

Fig. 1. DSC heating curves of (a) $LiPF_6$, (b) the fully lithiated graphite anode, (c) the fully lithiated graphite anode with 10 wt.% $LiPF_6$, (d) the fully lithiated graphite anode with 30 wt.% $LiPF_6$, (e) the enlarged profile of (a) and (f) the enlarged profile of (b).

charged to 0.01 V are shown in Fig. 2. The pronounced peaks at 1455 and 856 cm^{-1} in the lithiated graphite anode before heating are originated from the Li_2CO_3 generated by a direct two-electron reduction of ethylene carbonate (EC). The absorption peaks at 1630 and 1051 cm^{-1} are associated with lithium alkylcarbonates ($ROCO_2Li$), which are formed on the anode surface by a single electron electrochemical reduction of EC [15,16]. It is well known that the solid electrolyte interphase (SEI) layer is mainly composed of Li_2CO_3 and various lithium alkylcarbonates ($ROCO_2Li$) as well as small amounts of LiF, Li_2O, and LiOH formed by the electrolyte decomposition [17]. When the lithiated graphite anode (LiC6 + PVdF binder) without an electrolyte is heated in a DSC cell, five possible decomposition reactions generating the exothermic heat are as follows:

- Thermal decompositions of the meta-stable compounds like lithium alkyl carbonate in the presence of the lithiated graphite anode ($2Li + (CH_2OCO_2Li)_2 \rightarrow 2Li_2CO_3 + C_2H_4$, $ROCO_2Li \rightarrow R^\bullet + H^\bullet + Li_2CO_3$, and $R^\bullet + O_2 \rightarrow ROO^\bullet + H^\bullet \rightarrow ROOH$).
- Thermal reaction of PF_5 (generated from $LiPF_6$ decomposition) with the intercalated Li ions ($Li + PF_5 \rightarrow Li_{1-x}PF_{5-x} + xLiF$).
- Thermal reactions of OPF_3 and PF_5 (generated from $LiPF_6$ decomposition) with organic compounds in the SEI layer ($OPF_3 + ROCO_2Li \rightarrow OP(R)_{1-x}F_x + Li_2CO_3$).

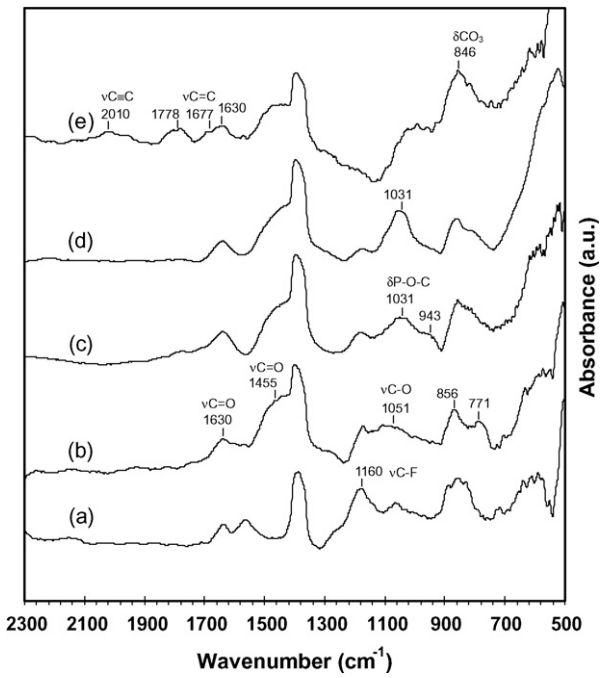

Fig. 2. FT-IR spectra of (a) non-cycled graphite anode, (b) the fully lithiated graphite anode before heating, heated to (c) 200, (d) 275 and (e) 400 °C.

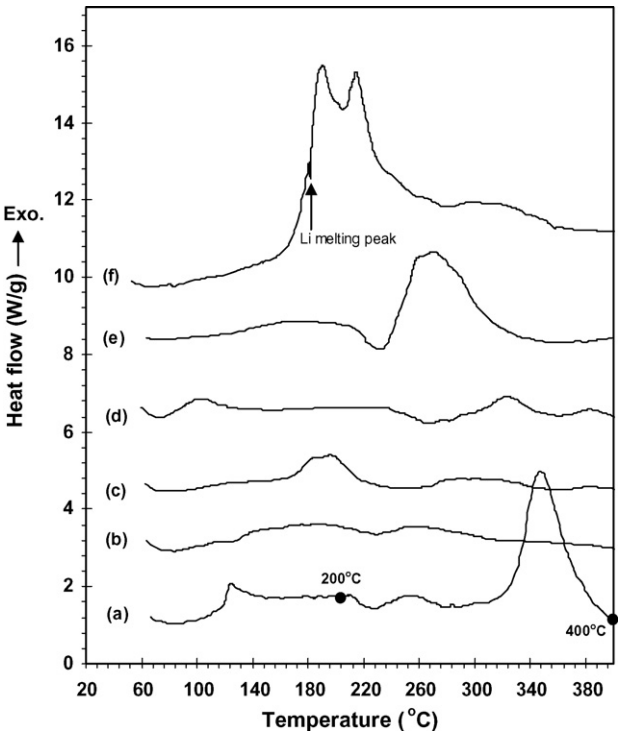

Fig. 3. DSC heating curves of (a) the fully lithiated graphite anode with EC:EMC (3:7)/1.3 M $LiPF_6$, (b) LiF with EC:EMC (3:7)/1.3 M $LiPF_6$, (c) $Li_2C_2O_4$ with EC:EMC (3:7)/1.3 M $LiPF_6$, (d) Li_2CO_3 with EC:EMC (3:7)/1.3 M $LiPF_6$, (e) EC:EMC (3:7)/1.3 M $LiPF_6$ and (f) Li metal with EC:EMC (3:7)/1.3 M $LiPF_6$.

- Thermal reaction of HF (generated from $LiPF_6$ decomposition) with Li_2CO_3 in the SEI layer ($HF + Li_2CO_3 \rightarrow LiF + H_2CO_3$).
- Thermal reaction of HF generated from a PVdF binder with intercalated Li ions ($-CH_2-CF_2- \rightarrow -CH{=}CF- + HF$, $HF + Li \rightarrow LiF + 1/2H_2$).

New peaks assigned to the P–O–C antisymmetric stretching and the P–OH stretching in the phosphorous compounds appeared at 1031 and 943 cm^{-1} in the FT-IR spectrum obtained after heating the lithiated graphite anode up to 200 °C (Fig. 2(c)) [18]. The intensity of the peak assigned to the phosphorous compounds (1031 cm^{-1}) increased while heating the lithiated graphite anode up to 275 °C (Fig. 2(d)). It was reported that PF_5 (g) formed via the thermal decomposition of $LiPF_6$ reacts with protic impurities like ROH and water to generate phosphorous oxyfluoride (OPF_3) [19]. OPF_3 can react with carbonate-containing compounds to produce P–O–C and P–OH bonds. Indeed, the lithiated graphite anodes after adding 10 and 30 wt.% $LiPF_6$ showed distinct and large exothermic peaks at 258 and 266 °C, respectively, as illustrated in Fig. 1(c) and (d). The increase of LiPF6 amount led to the argumentation of the peak intensity. The $LiPF_6$ trapped in the SEI layer during the charging process thermally decomposes into LiF (s) and PF_5 (g) at around 200 °C. The PF_5 (g) generated in a sealed DSC pan simultaneously produces OPF_3 and HF by reaction with water traces. It is plausible that highly reactive compounds (such as PF_5, OPF_3, and HF) react simultaneously with the metastable decomposition products in the SEI layer and thereby amplify the exothermic heat. A small exothermic peak around 310 °C in Fig. 1(c) seems to correspond to the thermal decomposition of the PVdF binder and this point could be confirmed from the FT-IR results. The C–F stretching peak of the PVdF binder (1160 cm^{-1}) almost disappeared after heating the lithiated graphite anode up to 400 °C. In addition, new peaks assigned to the C=C, C=O, and C≡C stretching were observed at 1677, 1778, and 2010 cm^{-1}, respectively, in Fig. 2(e). The formation of unsaturated carbon–carbon bonds in halogenated hydrocarbons occurs by dehydrohalogenation, namely the elimination of a hydrogen and a halogen atom from two adjacent carbon atoms [20]. This result is in agreement with work by Tarascon's group [21]. The carbon–carbon triple bonds are formed by elimination of HF from the $-CH_2-CF_2-$ bond in the PVdF binder in the presence of lithiated graphite at high temperatures. We think that the reaction of HF produced via the dehydrohalogenation of a PVdF binder with intercalated Li ions contributes to the exothermic heat around 325 °C.

Fig. 3 shows the DSC heating curves for EC/EMC (3/7)/1.3 M $LiPF_6$, for a lithiated graphite anode, a Li metal, LiF, $Li_2C_2O_4$ (lithium oxalate), and Li_2CO_3 in presence of an electrolyte solution. The DSC curves for the lithiated graphite anode with and without electrolyte are quite different as shown in Figs. 1(b) and 3(a), respectively. It can clearly be seen that results for the lithiated graphite anode without EC/EMC/1.3 M $LiPF_6$ do not indicate the onset of an exothermic peak at 90 °C. Yamaki et al. reported that the first exothermic peak around 140 °C is caused by the reaction (SEI formation) of an electrolyte and a lithiated graphite, whose surface is covered by PVdF binder without formation of SEI. DSC measurements were carried out for Li metal with EC/EMC 1 M $LiPF_6$ to identify this point. There is no peak around 140 °C, as shown in Fig. 3(f). The exothermic heat generation began at 140 °C and two peak temperatures were 190 and 215 °C. This indicates that these two exothermic peaks are ascribed to the thermal reactions (SEI formation) of the electrolyte and the Li metal. It should be noted that the reactivity of Li metal is analogous with lithiated graphite. From this result, we can say that the first exothermic peak at 120 °C in Fig. 3(a) is not produced by the reaction of an electrolyte with a lithiated graphite. In order to characterize this exothermic peak, a FT-IR spectrum of the lithiated graphite with electrolyte heated up to 200 °C was obtained. It is difficult to accurately identify the $ROCO_2Li$ peak because $ROCO_2Li$ actually represents a series of lithium alkyl carbonates. It should be noted that their peak positions depend on the R group and are determined by the SEI layer structure. The relative intensities of the peaks assigned to lithium alkyl carbonates ($ROCO_2Li$) (1630–1635, 1434,

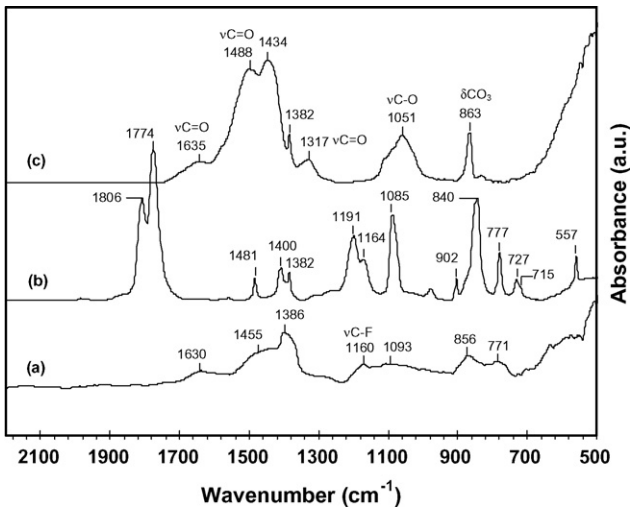

Fig. 4. FT-IR spectra of the fully lithiated graphite anode with EC:EMC (3:7)/1.3 M $LiPF_6$ (a) before heating (no electrolyte), heated to (b) 200 and (c) 400 °C.

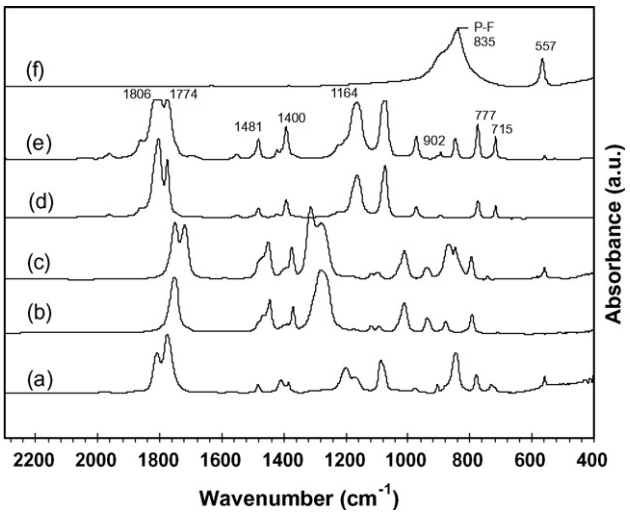

Fig. 5. FT-IR spectra of (a) the fully lithiated graphite anode with EC:EMC (3:7)/1.3 M $LiPF_6$ (heated up to 200 °C), (b) EMC, (c) EMC/1.3 M $LiPF_6$, (d) EC, (e) EC/1.3 M $LiPF_6$ and (f) $LiPF_6$.

1317 and 1051 cm^{-1}), the lithium oxalate ($Li_2C_2O_4$) peaks (1630, 1320 and 770–780 cm^{-1}), and the Li_2CO_3 peaks (1455, 856 cm^{-1}) decreased remarkably, as shown in Fig. 4(a) and (b). This means that various lithium alkyl carbonates, $Li_2C_2O_4$, and Li_2CO_3 present in the SEI layer thermally decompose upon heating up to 200 °C and then form new compounds. Free radicals ($R^•$, $H^•$) are produced by the thermal decomposition reactions of lithium alkyl carbonates ($ROCO_2Li$ in the SEI layer → $R^• + H^• + Li_2CO_3$) at high temperatures and a recombination of these radicals with protic compounds (EC, EMC, water trace, etc.) in the electrolyte occurs, resulting in the production of exothermic heat. To clarify the thermal reactions between SEI and an electrolyte, DSC measurements for main components in SEI with an electrolyte were carried out. Fig. 3(c) and (d) exhibit that $Li_2C_2O_4$ and Li_2CO_3 reported as important components in SEI [22] thermally decompose around 195 and 105 °C, respectively. This result can successfully rationalize that $Li_2C_2O_4$ and Li_2CO_3 react with HF generated from $LiPF_6$ in an electrolyte ($Li_2C_2O_4 + 2HF \rightarrow 2LiF + H_2C_2O_4$, $Li_2CO_3 + 2HF \rightarrow 2LiF + H_2CO_3$) and their peaks in Fig. 4(a) and (b) are reduced via these reactions. LiF formed by the electrochemical decomposition of $LiPF_6$ did not show significant exothermic peaks except for two broad exothermic peaks produced by the electrolyte decomposition in Fig. 3(b). The comparison of Fig. 3(a) and (d) manifests that the first exothermic peak around 120 °C is attributed to the thermal reactions between Li_2CO_3 in SEI and an electrolyte in presence of a lithiated graphite anode. We think that the schematic model for the thermal reactions of SEI with an electrolyte proposed by Dahn's group is appropriate to explain the exothermic peak around 120 °C [23].

Fig. 5 shows the FT-IR spectra for the organic solvents, the electrolyte solutions, and $LiPF_6$. There are no peaks related to EMC in the lithiated graphite anode with electrolyte heated at 200 °C. Sharp peaks in Fig. 4(b) are assigned to the solvated EC interacting with Li^+ ions (1806, 1774, 1481, 1400, 1164, 902, 777 and 715 cm^{-1}) and the $LiPF_6$ salt (835 and 557 cm^{-1}). This implies that the EMC solvent, having a low boiling point of 108 °C, is evaporated from the lithiated graphite anode with electrolyte upon the heating up to 200 °C and disappears after the disassembling of the DSC cells. Fig. 6 shows the FT-IR spectra for the region of the EC ring-breathing mode. It is found that a peak corresponding to free EC (893 cm^{-1}) was absent in the lithiated graphite anode with electrolyte heated at 200 °C. This indicates that all the EC molecules participate in the dissociation of $LiPF_6$ due to the evaporation of EMC.

The two broad exothermic peaks between 180 and 300 °C seem to be the result of the thermal decompositions of EC/EMC (3/7)/1.3 M $LiPF_6$ as shown in Fig. 3(a) and (e). Finally, in order to characterize the onset of the large exothermic peak at 300 °C, FT-IR measurements were performed for the lithiated graphite anode with electrolyte heated at 400 °C. The C–F stretching peak of the PVdF binder (1160 cm^{-1}) was not observed in Fig. 4(c) and this result was in accordance with that of an electrolyte-free lithiated graphite. In addition, the peaks assigned to lithium alkylcarbonates ($ROCO_2Li$) (1635, 1434, 1317 and 1051 cm^{-1}) and Li_2CO_3 peaks (1488 and 863 cm^{-1}) prominently increased. After two large exothermic peaks with the onset around 140 °C appear, the broad exothermic peak around 300 °C is shown in Fig. 3(f). This indicates that SEI formation begins at 140 °C via the thermal reactions of an electrolyte with a Li metal and continues until 380 °C. It is believed

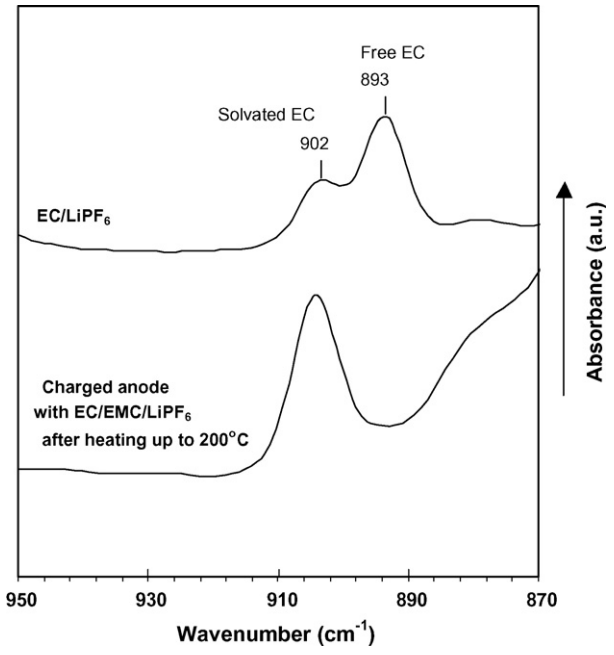

Fig. 6. FT-IR spectra for the ring breathing mode of EC in EC/1.3 M $LiPF_6$ and charged graphite anode with EC:EMC (3:7)/1.3 M $LiPF_6$ heated to 200 °C.

that the thermal decomposition reactions of organic solvents and $LiPF_6$ with a lithiated graphite continue from 200 to 400 °C and that a large amount of $ROCO_2Li$ and Li_2CO_3 is thereby produced. It can be concluded from these results that the exothermic peak around 350 °C is caused by the SEI formation (lithium alkylcarbonates, Li_2CO_3) and the thermal decomposition reactions of the PVdF binder with the lithiated graphite.

4. Conclusions

The thermal and spectral studies of a lithiated graphite anode, with and without electrolyte, clearly showed that the SEI layer, the $LiPF_6$-based electrolyte, and the PVdF binder on the lithiated graphite anode thermally decompose at high temperatures. Moreover, it could be confirmed that the PF_5 formed by the thermal decomposition of $LiPF_6$ reacts with ROH in the SEI layer and that this reaction leads to the formation of phosphorous compounds on the lithiated graphite anode surface at around 200 °C. The presence of the electrolyte led to thermal decomposition reactions of the SEI layer on the lithiated graphite anode at a low onset temperature around 90 °C.

Acknowledgement

The authors would like to thank Samsung SDI Corporation for the support of this work.

References

[1] P.G. Balakrishnan, R. Ramesh, T.P. Kumar, J. Power Sources 155 (2006) 401–414.
[2] Ph. Biensan, B. Simon, J.P. Pérès, A.d. Guibert, M. Broussely, J.M. Bodet, F. Perton, J. Power Sources 81/82 (1999) 906–912.
[3] H. Yang, G.V. Zhuang, P.N. Ross Jr., J. Power Sources 161 (2006) 573–579.
[4] X.G. Teng, F.Q. Li, P.H. Ma, Q.D. Ren, S.Y. Li, Thermochim. Acta 436 (2005) 30–34.
[5] Z. Zhang, D. Fouchard, J.R. Rea, J. Power Sources 70 (1998) 16–20.
[6] T. Kawamura, A. Kimura, M. Egashira, S. Okada, J. Yamaki, J. Power Sources 104 (2002) 260–264.
[7] K. Edström, A.M. Andersson, A. Bishop, L. Fransson, J. Lindgren, A. Hussénius, J. Power Sources 97/98 (2001) 87–91.
[8] J. Yamaki, H. Takatsuji, T. Kawamura, M. Egashira, Solid State Ionics 148 (2002) 241–245.
[9] A.M. Andersson, K. Edström, J.O. Thomas, J. Power Sources 81/82 (1999) 8–12.
[10] J. Yamaki, Y. Baba, N. Katayama, H. Takatsuji, M. Egashira, S. Okada, J. Power Sources 119–121 (2003) 789–793.
[11] H. Yang, X.D. Shen, J. Power Sources 167 (2007) 515–519.
[12] H. Maleki, G. Deng, A. Anani, J. Howard, J. Electrochem. Soc. 146 (1999) 3224–3229.
[13] B. Ravdel, K.M. Abraham, R. Gitzendanner, J. DiCarlo, B. Lucht, C. Campion, J. Power Sources 119–121 (2003) 805–810.
[14] Z. Lu, L. Yang, Y. Guo, J. Power Sources 156 (2006) 555–559.
[15] R. McMillan, H. Slegr, Z.X. Shu, W. Wang, J. Power Sources 81/82 (1999) 20–26.
[16] P.B. Balbuena, Y. Wang, Lithium-Ion Batteries: Solid-Electrolyte Interphase, Imperial College Press, London, 2004, pp. 255–260.
[17] H. Ota, Y. Sakata, Y. Otake, K. Shima, M. Ue, J. Electrochem. Soc. 151 (11) (2004) A1778–A1788.
[18] J.B. Lambert, H.F. Shurvell, D.A. Lightner, R.G. Cooks, Introduction to Organic Spectroscopy, Macmillan Publishing Company, A division of Macmillan, Inc., 1976, p. 217.
[19] C.L. Campion, W. Li, B.L. Lucht, J. Electrochem. Soc. 152 (12) (2005) A2327–A2334.
[20] J. March, Advanced Organic Chemistry, McGraw-Hill, New York, NY, 1977, p. 935.
[21] A. Du Pasquier, F. Disma, T. Bowmer, A.S. Gozdz, G. Amatucci, J.-M. Tarascon, J. Electrochem. Soc. 145 (1999) 472–477.
[22] G.V. Zhuang, H. Yang, B. Blizanac, P.N. Ross Jr., Electrochem. Solid-State Lett. 8 (2005) A441–A445.
[23] M.N. Richard, J.R. Dahn, J. Electrochem. Soc. 146 (1999) 2068–2077.